



Fire resistance of composite non-load bearing light steel framing walls

Journal of Fire Sciences

1–20

© The Author(s) 2020

Article reuse guidelines:

sagepub.com/journals-permissions

DOI: 10.1177/0734904119900931

journals.sagepub.com/home/jfs

Seddik M Khetata¹ , Paulo AG Piloto² and Ana BR Gavilán³

Date received: 4 September 2019; accepted: 25 December 2019

Abstract

The light steel frame walls are mostly used for non-load bearing applications. The light steel framed walls are made with studs and tracks that require fire protection, normally achieved by single plasterboard, by composite protection layers or by insulation of the cavity. The partition walls are fire rated to resist by integrity and insulation. Seven small-scale specimens were tested to define the fire resistance of non-load bearing light steel frame walls made with different materials. All tests were validated using two-dimensional numerical models, based on the finite-element method, the finite-volume method and hybrid finite-element method. A good agreement was achieved between the numerical and the experimental results from fire tests. The fire resistance increases with the number of studs and also with the thickness of the protection layers. The hybrid finite-element method solution method looks to be the best approximation model to predict fire resistance.

Keywords

Fire tests, light steel frame walls, composite layers, numerical simulation, fire resistance

Introduction

The light steel frame (LSF) construction technology started to be used in different types of buildings, replacing the traditional construction methods due to its light-weight characteristics. Steel is recycled, dimensional stable, and ease of installation. LSF and prefabricated

¹Department of Mechanical Engineering, University of Salamanca, Salamanca, Spain

²Department of Applied Mechanics, Polytechnic Institute of Bragança, Bragança, Portugal

³Department of Mechanic Engineering, University of Salamanca, Zamora, Spain

Corresponding author:

Seddik M Khetata, Department of Mechanic Engineering, University of Salamanca, 37008 Salamanca, Spain.

Email: s.khetata@usal.es

panels are most used in non-load-bearing walls. The LSF walls are made with studs and tracks that require fire protection, normally achieved by a single plasterboard, by composite protection layers, or by insulation of the cavity. The insulation capacity (I) is the ability of the construction element to withstand fire exposure by one side, without the transmission of significant heat to the unexposed side. Seven small-scale fire tests were developed to define the fire resistance according to EN 1363-1¹ and EN 1364-1,² with the main objective to evaluate the influence of the protection layers and the influence of the cavity insulation materials. Numerical models are also validated with experimental tests.

Different studies and investigations were developed with the aim of testing the influence of using different configurations of LSF walls, different protection materials such as plasterboards and insulation materials. One of the first research in this domain was developed at the Cornell University in 1963 by G. Winter, which did several analyses on the effects of cold-straining on structural sheet steels, including the corner properties of cold-formed steel shapes, the effects of cold-forming on the mechanical properties and on structural behaviour of members.³ In 1973, Son and Shoub⁴ developed two fire-endurance tests on symmetric double-wall assemblies, the first specimen was made using cold-rolled steel 'C'-type studs, welded to tracks, and the cavity was fulfilled by the glass fibre covered by gypsum board type X. The second specimen used rectangle hollow section studs and thicker insulation material in the cavity, with the aim to improve the fire resistance. The second tests led to better fire endurance in load domain. The temperature data for the second test also indicated a much slower temperature rise in the unexposed gypsum board, and a better solution in practice would be the use of a two-layer construction plates with staggered application of board joints to eliminate direct heat access to the steel studs in joints. Kenneth J. Schwartz and T. T. Lie⁵ in 1985, studied the effect of the heat transmission to prevent ignition of the materials in contact with the unexposed side of the partition wall. Authors analysed data from previous experimental tests and made more experiments to evaluate the insulation criteria of the American standard ASTM E119. The information helped to understand the relationship between the unexposed surface temperature rise criteria and the ignition temperature of common combustible materials. In 2000, Alfawakhiri and Sultan⁶ presented a comparison between experimental tests and numerical models, demonstrating how different heating regimes applied in cold-formed steel studs cause different structural failure modes. An experimental investigation was also developed by Ghazi Wakili and E. Hugi⁷ in 2009, dealing with thermal properties of the materials and comparing the fire behaviour of four types of gypsum materials, investigating the temperature history evolution for a box-protected steel column, finding more than 100°C of maximum difference on the steel temperature after 90 min of fire exposure, when considering different types of gypsum materials. In 2014, Nassif et al.⁸ published results of several full-scale fire tests on the steel-stud gypsum-faced partition wall. The results were used to verify the numerical procedure to be used in predicting the thermo-mechanical behaviour. The measured temperatures across the wall agreed with the predicted values until the falling off of the gypsum board. Jonathan Vallée⁹ in 2016 developed numerical validations, using ABAQUS and fire dynamic simulator (FDS) to simulate furnace tests developed for LSF partition walls, testing empty cavities, and insulated cavities. Author concluded that insulation material in the cavity can improve the fire resistance, when considering the insulation criterion, especially when ablation of the gypsum plates occurs. Dias et al.¹⁰ in 2019 presented the results of 13 small-scale fire tests conducted on non-load-bearing steel and gypsum plasterboard sheathed panels and walls, and numerical simulations were conducted to evaluate the enthalpies of plasterboards and steel

sheathing. They concluded that retention of vaporised water from the calcination process within the plasterboard due to the confinement provided by steel sheathing is a crucial factor that improves the fire performance of such walls.

The fire performance on non-load-bearing LSF walls started to be investigated in 2017 at the Polytechnic Institute of Bragança (IPB) with the aim of (1) developing accurate numerical models based on the thermal analysis with fluid structure interaction;¹¹ (2) validating the numerical models with tests performed by others;¹² (3) analysing the fire performance of LSF using the simplified one-dimensional heat flow;¹³ (4) presenting a sequential numerical model to study the fire resistance of LSF walls made with composite panels under load-bearing conditions¹⁴ and; and (5) predict the load effect on the LSF walls under fire conditions using numerical simulations.¹⁵ In 2019, nine experimental fire tests were developed to define the fire resistance of the partition walls, and compare the behaviour of composite plates with the traditional solution using gypsum protection plates. These tests were simulated with three-dimensional (3D) finite-element models using ANSYS¹⁶ applying the hybrid solution method FEM-H for nonlinear thermal analysis. The numerical results agree well with the experimental results, for all the measured quantities, including the maximum and average temperature for the unexposed surface. The maximum difference for the fire resistance is below 12%, for most of the specimens.¹⁷

This investigation is related with the fire resistance for insulation of non-load-bearing walls made with LSF protected with composite layers. Three different LSF structures are presented (3, 4 and 5 studs) along with two insulation materials for the cavity (rockwool and ceramic fibre) and different materials for the composite layers (gypsum, cork and oriented strand board (OSB)). The reduced scale of the testing assemblies was able to capture most of the mechanical and thermal effect that can lead to the thermal failure of the LSF wall. Due to the restraining conditions of the wall inside the furnace frame and the effect of the thermal expansion, the LSF structure was compressed in the main directions of the studs, leading to the typical instability buckling modes (global and local). Due to the heating effect, large cracks are expected on the gypsum plates, both horizontally and vertically. The main purpose of this investigation is to determine the fire resistance of the composite LSF wall assemblies and to compare with the fire resistance of traditional solutions (gypsum boards). Temperature readings were collected with a frequency of 1 Hz, in different points inside the wall and in the unexposed side of the wall, getting data for the validation of the computer models. Special measurements were defined to detect the thermal degradation of materials and the penetration of flames and hot gases in the cavity. Due to the limitations of the furnace, the specimens were sized to fit the furnace frame, which do not present the real dimensions required by the standard EN 1364-1² in fire tests, but provide important results for the behaviour of materials and structures. All the other conditions specified in this standard were met, as well as the general requirements for standard fire tests EN 1363-1.¹

Fire tests

Conditions and criteria

Seven small-scale LSF walls were tested in a small fire-resistance furnace. This furnace is able to follow the standard fire ISO834 condition (International Organisation for Standardisation, 1999).¹⁸ A plate thermocouple is included inside the furnace to control the gas temperature. This furnace is running on natural gas, using four burners separated apart

in height and depth, each with 90 kW of maximum power. The dimensions of the furnace are $1\text{ m} \times 1\text{ m} \times 1\text{ m}$, prepared with frontal door to setup the frame with the testing specimens. The generic standard EN 1363-1¹ and the specific standard EN 1364-1² were used to define the fire resistance of the seven non-load-bearing walls. The fire resistance is the ability of the element to withstand exposure to fire only on one side, without significant heat transfer from the exposed side to the unexposed side. The heat transfer should be limited to avoid that the unexposed surface or any material close to that surface is ignited. The fire resistance of a partition wall should be defined based on the shortest time for which the criteria of maximum or the average temperature increase are satisfied in any discrete area. The fire performance level used to define the insulation shall be calculated on the basis of the increase in the average temperature on the unexposed side, limited to 140°C above the initial average temperature, or, based on the increase of the maximum temperature in any location, limited to 180°C above the initial average temperature. Local measurements were developed by k-type thermocouple and field measurements by infrared thermography (IR). This field measurement (IR) was used to capture all the temperature values in the unexposed area, enabling big data for doing the calculation of the average and maximum temperature and supporting the identification of the critical region of the unexposed surface. According to our records, the maximum difference between the IR measurement and the single measurement (thermocouple) was 4%. The maximum difference for the maximum temperature was 16%. This bigger difference may be explained due to the fact that the maximum temperature appears to be achieved in the screw regions. For this reason, only the average IR measurement will be presented for comparison.

Wall specimens

The fire tests were developed in the furnace at the IPB, see Figure 1. Different wall configurations were tested, using different number of studs and spacing in between, (see Table 1), different types of protection layers and two different insulation materials for the cavity. These LSF walls are made with cold-formed steel profiles forming a cavity thickness of 90 mm, using stud profiles $\text{C90} \times 43 \times 15 \times 1.5$ and track profiles $\text{U93} \times 43 \times 1.5$ (see Figure 1). The studs and tracks are pinned by using self-drilling screw with a diameter of 4.2 mm and length of 19 mm (position 0 in Figure 2). All profiles have the steel grade S280GD. The Class 3 OSB was selected for wall panelling with 10 mm thickness, being appropriate for structural applications on wet conditions. The agglomerated cork with polyurethane elastomer bonding agent was selected with 10 mm thickness, being normally used for acoustic and insulation applications. The Gypsum layer was selected, based on its fire resistance characteristics. The gypsum density at room temperature is 700 kg/m^3 , being formed by two sheets of multi-ply paper with the inner core made of high-purity gypsum reinforced by fibreglass filaments and properly additives with thermal expander minerals. The LSF structure was fixed to three edges of the furnace frame (left side, bottom and top) allowing a free edge, properly filled with ceramic fibre on the right side (gap size equal to 25 mm). All the wall borders were filled with gypsum-based product for closing the connection with the frame of the furnace. This product was received in powder state, ready to be mixed with water. The application can be seen in Figure 1.

The layer plates were fixed on both sides of the LSF structure, using different self-drilling screws (see position 1, 2 and 3 in Figure 2). The screws positioned on the external side of the wall (exposed and unexposed) were protected with gypsum. The wall Specimens 10 and 15

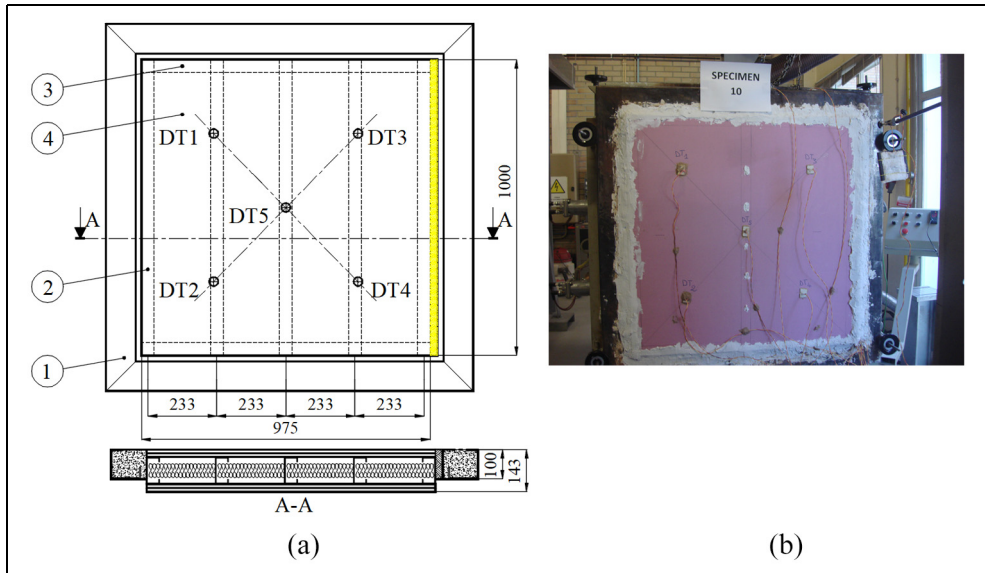


Figure 1. LSF wall specimen and testing frame (1). Vertical studs (2), horizontal tracks (3) and layer plates (4) and position of the disc thermocouples (DT_i) in the unexposed surface (dimensions in mm).

Table 1. LSF walls: Materials and geometry.

Specimen ID	LSF studs	Spacing (mm)	Cavity (kg/m ³)	Layer 1 (mm)	Layer 2 (mm)	Layer 3 (mm)
10	3	466	Rockwool/75	12.5 Gypsum F	–	–
11	3	466	–	12.5 Gypsum F	–	12.5 Gypsum F
12	3	466	–	12.5 Gypsum F	10 Cork aggl.	12.5 Gypsum F
13	5	233	–	12.5 Gypsum F	10 Cork aggl.	12.5 Gypsum F
14	5	233	–	10 (OSB 3)	12.5 Gypsum F	12.5 Gypsum F
15	3	466	Superwool/128	12.5 Gypsum F	–	–
16	4	487.5	Superwool/128	12.5 Gypsum F	–	–

were made with three studs – two tracks and one gypsum board fixed by five self-drilling screws with a diameter of 4.8 mm and length of 32 mm and each stud spaced every 152 mm (vertical direction), see screw position 1 in Figure 2. Four screws were included in the horizontal direction. For the other tests, the same self-drilling screws were used to fix the first plasterboard (position 1) and additional self-drilling screws with a diameter of 4.8 mm and length of 50 mm were used to fix the second gypsum layer (position 2). Self-drilling screws with 63 mm of length and 5.5 mm of diameter were used to fix the third layer in tests 12, 13 and 14, (position 3). All screws were spaced every 91 mm in vertical direction. More details about the distribution of the screws along the steel structure (studs and tracks) to fix the plasterboards and the number of protection layers are presented in Figure 2.

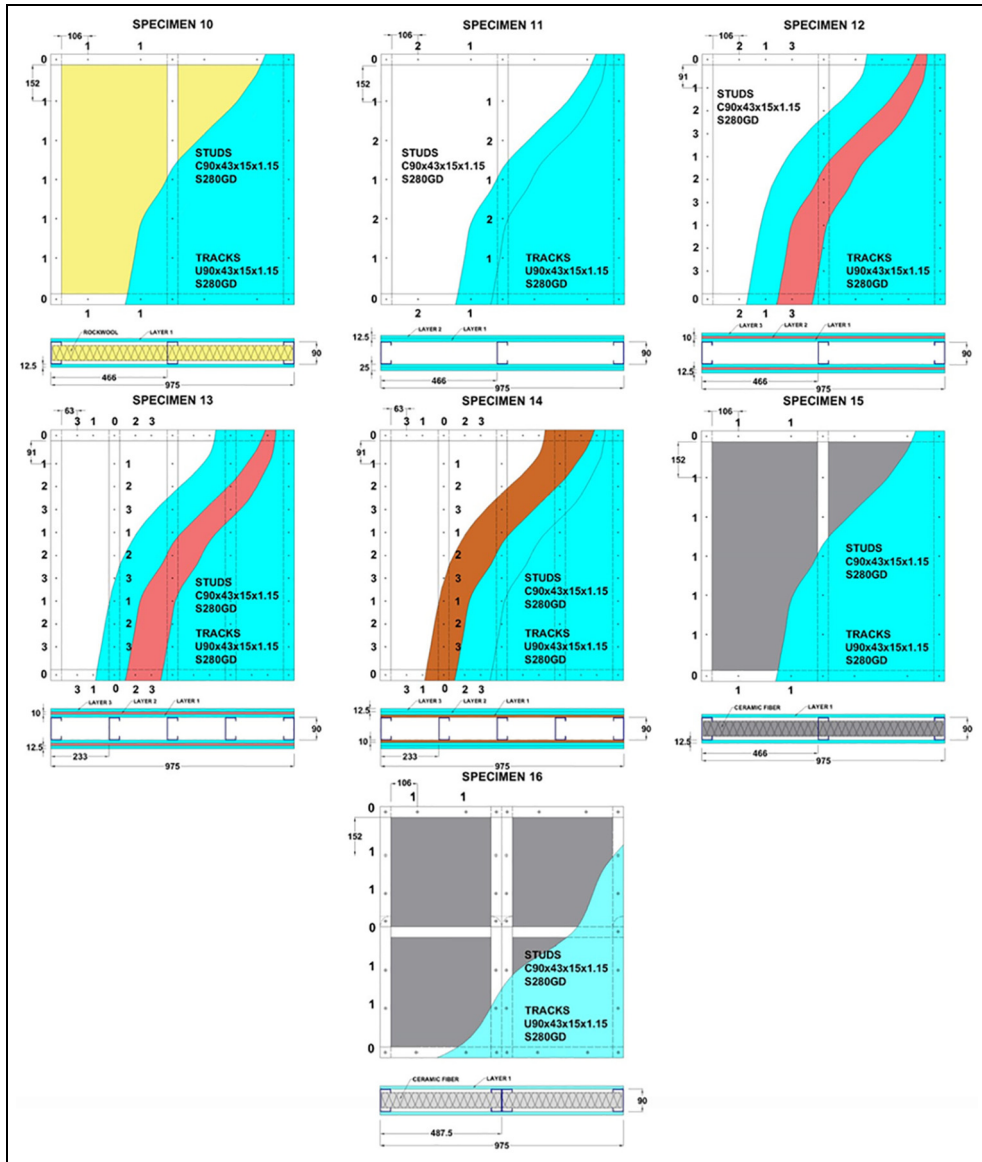


Figure 2. Specimen walls made with the LSF (dimensions in mm).

Instrumentation

Temperature was collected with 1 Hz frequency, using the HBM system MGCPlus. A total of 22 channels were used for the measurements. In addition, an infrared thermal camera FLIR BT Series T365, with the resolution of 320×240 pixels, was used to measure the unexposed temperature field, using the acquisition frequency set to 1.25 Hz, with a fixed-scale temperature between 15°C and 250°C . Several type-K thermocouples with diameter of 0.7 mm were attached into the specimen, with different formats for temperature

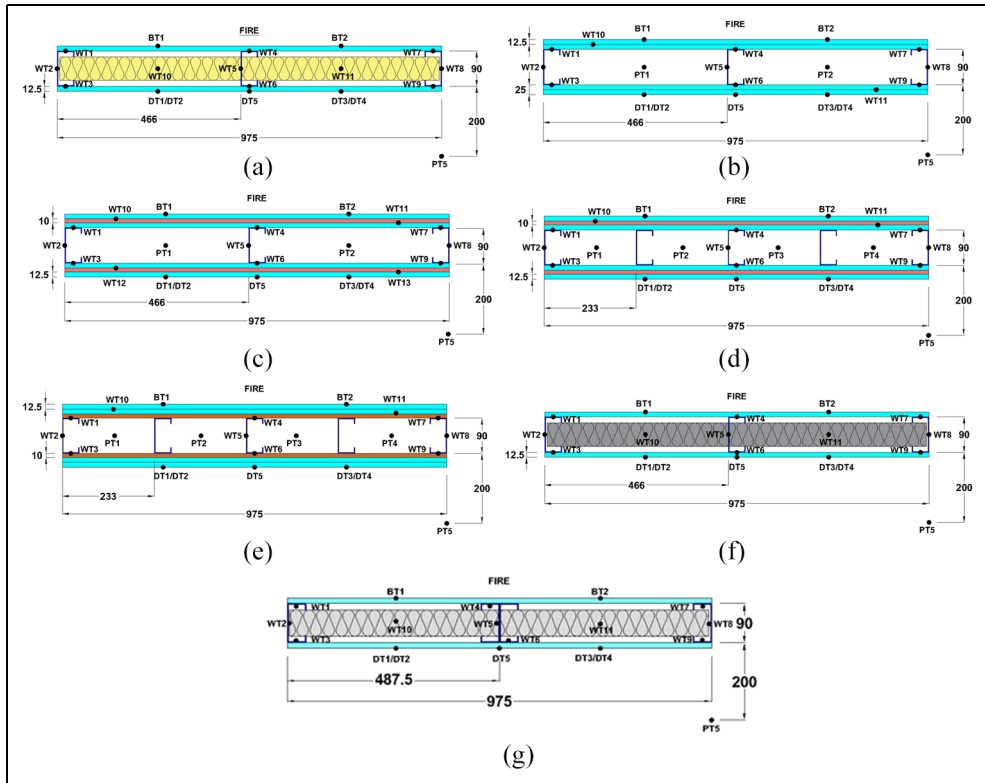


Figure 3. Specimens and thermocouples position: (a) Specimen 10, (b) Specimen 11, (c) Specimen 12, (d) Specimen 13, (e) Specimen 14, (f) Specimen 15, and (g) Specimen 16.

measurement: copper disc with plasterboard protection (DT_i) for measuring the unexposed surface temperature; plate thermocouples (PT_i) facing the unexposed side were fixed at the mid height of the cavity to determine the average temperature (CAV) and also the ambient temperature (located 200 mm away from the unexposed surface); the hot joint made with twisted thermocouples cables (WT_i) were used to measure the temperature in between plates and inside the insulation material when applied in cavity; welded hot joint were applied on cold-formed steel profiles (WT_i) and used for measuring the temperature of the steel parts (hot flange-HF, web-WEB and cold flange – CF); sheath thermocouples (BT_i) were used for measuring the temperature on the exposed surface. More detailed information can be found in study of Piloto and colleagues.¹⁹

The number and distribution of thermocouples depends on the configuration of the wall specimen, in particular depends on the number of studs, see in Figure 3.

Fire tests results

Different instability modes of the LSF were achieved during the test, due to local and global buckling deformed shapes. These ultimate limit states of the LSF frame are due to the

thermal expansion of each steel member because the LSF is fixed on three edges to the frame of the furnace. The insulation criterion has been used to define the fire resistance, so failure is expected by the attainment of the temperature criteria in the unexposed surface. For the Specimens 12, 13 and 14, the furnace temperature goes beyond the standard temperature ISO 834 due to the heat release effect of the combustible materials (cork and OSB). The lack of combustible materials in the layered wall specimens explains the proximity of the furnace temperature with the ISO 834 curve, see Figure 4. The temperature history is presented with average values for some important regions on the left side in Figure 4, while the temperature field is presented on the right side for a specific time during the test. The IR results in Figure 4 allows to compare the temperature field after 110 min of fire exposure. These infrared thermal images allow to identify the position of the LSF frame, the position of the screws and the first cavity or region to lose integrity (E).

The maximum and average temperature of the unexposed side was determined using disc thermocouples UNEX (DT), obtained from the individual measurements of DT_i [1] and with a FLIR infrared thermal camera, located at 3-m distance from the unexposed surface, UNEX (IR). Special measurements were also defined for the specimens, such as: the average temperature of the cavity (CAV), obtained from the individual measurements of PT_i ; the room temperature (AMB) measured 200 mm away from the unexposed side of the LSF wall and the interface temperature (PB_i – PB_j) between the composite layered plates, obtained from the individual measurements of WT_i . The failure time is presented for the average temperature of the unexposed surface using Infrared thermography ($IR_{ave} = 140 + 20^\circ\text{C}$ (initial average temperature equal to 20°C), for the maximum temperature measured by the disc thermocouples ($DT_{max} = 180 + 20^\circ\text{C}$) and for the average temperature measured by the disc thermocouples ($DT_{ave} = 140 + 20^\circ\text{C}$) from the unexposed surface. The critical time for the mechanical resistance is also presented for the steel members, considering the average temperature from the three stud's main regions (hot flange – HF, web = WEB, and cold flange-CF) using single measurements, see Table 2. The critical temperature for the steel members can only be applicable for the case of load-bearing members (Class 4 cross-sections), if at time 't' the steel temperature at all cross-sections is not more than 350°C , according to the EN 1993-1-2.²⁰ This critical temperature criterion is sometimes overconservative for lower load levels and sometimes unsafe for higher load level.¹⁵ Despite being used for load-bearing walls, this criterion has been used for comparison with the temperature measured for the steel stud on the hot flange (HF), web (WEB) and cold flange (CF). It is also assumed that there is no direct effect of the mechanical load in the temperature field, reason why this temperature field may also be expected for load-bearing walls.

Figure 5 presents the final state from of the LSF walls, to better understand the major events during the tests. The brittle behaviour of the gypsum layer can be verified during and after the end of the test for all specimens. The gypsum plates lose their integrity by the existence of vertical and horizontal cracks. These patterns seem to be aleatoric, and the falling down side depend on the existence of insulation material in the cavity. The existence of insulation material in the cavity forces the gypsum plate to bend inside the furnace. The ignition of the combustible material was also detected during the tests of the Specimens 12, 13 and 14. Figure 5 also presents deformed configuration of the LSF structure. All specimens presented local instabilities (distortional and web buckling modes) due to the stud restrain in the vertical direction. Specimens 12–15 also present global instability in the unrestrained studs. Specimen 16 did not present any global mode of instability due to the existence of the

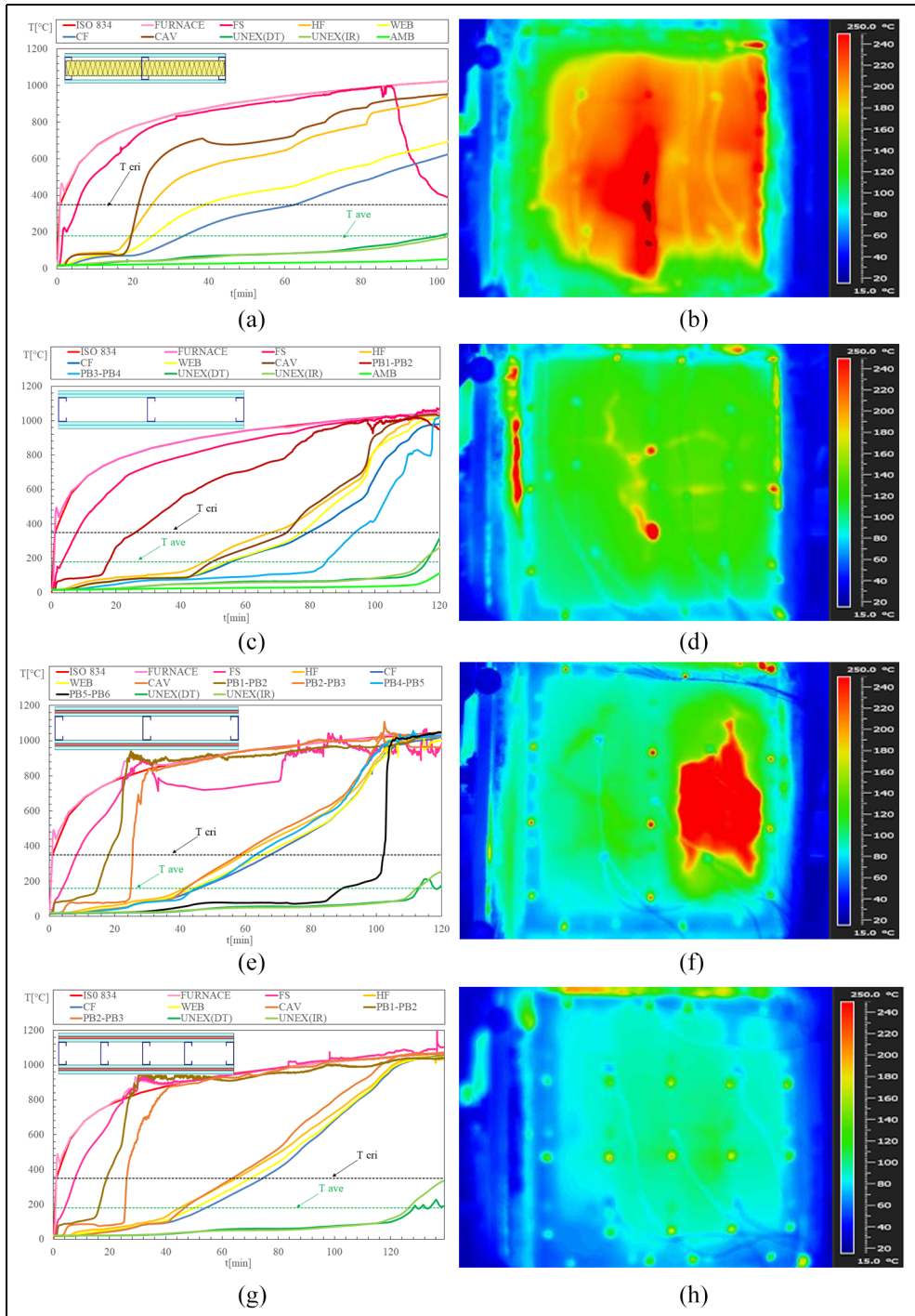


Figure 4. Continued

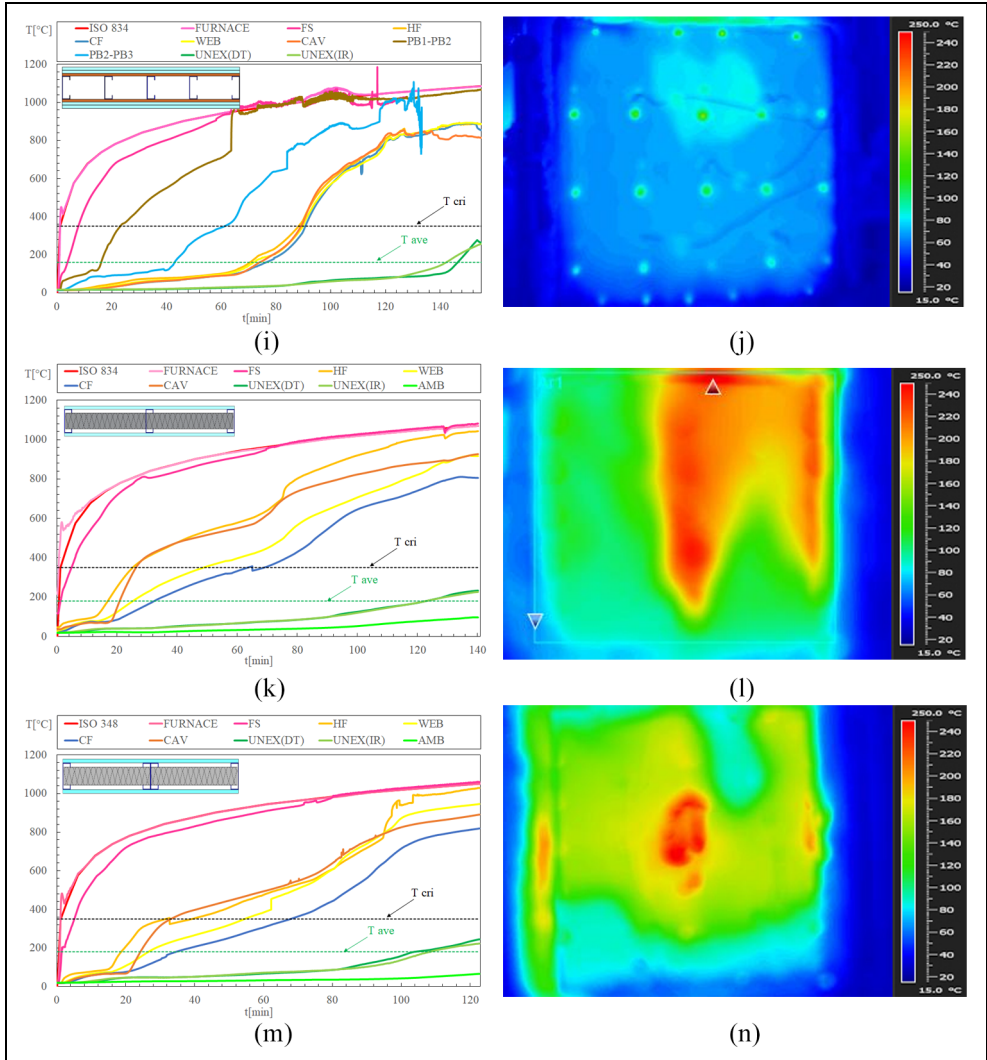


Figure 4. Temperature results on LSF wall specimens and Infra Red Temperature field after 110 minutes: (a, b) Specimen 10; (c, d) Specimen 11; (e, f) Specimen 12; (g, h) Specimen 13; (i, j) Specimen 14; (k, l) Specimen 15; (m, n) Specimen 16.

intermediate track. These buckling modes were expected due to the restraint level of the wall into the frame of the furnace.

The highest fire resistance was determined using the assembly of the Specimen 14. The OSB plate increases the stiffness of the protection layers, providing the geometric stability of the gypsum layers. This solution reached the critical time of 145 min. The worst solution seems to be that corresponding to Specimen 10, reaching the critical time of 79 min.

Table 2. Critical time for each tested specimen (fire resistance for insulation criteria (I) in completed minutes and fire resistance for steel elements of Class 4 (R)).

Specimen ID	DT _{max} (I) min	DT _{ave} (I) min	IR _{ave} (I) min	HF = 350°C min	WEB = 350°C min	CF = 350°C (R) min
10	79	95	99	25	39	62
11	114	115	113	68	79	77
12	112	113	112	59	65	67
13	122	127	125	65	70	74
14	145	146	142	88	90	91
15	95	115	115	25	48	63
16	86	100	104	39	54	67

The best insulation material seems to be the superwool. The diffusivity of the rockwool is higher than the diffusivity of the superwool for every temperature level. This justifies the higher fire resistance of Specimen 15 when compared with the Specimen 10.

Numerical validation

Solution methods and models

Three different two-dimensional (2D) numerical solution methods were used to simulate the seven fire tests of the non-load-bearing LSF wall. All the models assume perfect contact between materials. The first solution method (Solution Method 1) uses thermal and fluid interaction for both parts, solid and fluid, using the finite-volume method (FVM). The flow analysis considers laminar fluid and is based on density variation. The fluid motion is induced by heat transfer, and the solution is transient and nonlinear. The density-based solver solves the governing equations of continuity, momentum, and energy simultaneously. Pressure is obtained through the equation of state. Governing equations for additional scalars are solved afterward and sequentially (radiation). The integration time for each time step was 60 s, with the possibility to be reduced to 5 s. The convergence criterion was based on the residuals for each equation. The numerical model divides the cross-section in finite cells. The domain variables (pressure, velocity and temperature) are calculated in each cell, at the same time. The grid for all the domains (solid and fluid) of Specimen 11 is presented in Figure 6(b), using the minimum cell size equal to 0.0005 m. Only a small part of the model is represented to better understand the size of the grid. The second solution method (Solution Method 2) uses FEM and considers only the thermal analysis for solids, assuming perfect contact between materials. The transient and nonlinear thermal analysis was selected, with full option solution method. The same time step was used with similar convergence criterion for the heat flow. Figure 6(a, f, g) represents the mesh used for test 10, 15 and 16. The third solution method (Solution Method 3) uses the H-FEM to simulate test Specimens 12, 13 and 14 with special information coming from experimental results (average PT_i values (CAV) from the test are assumed inside the cavity). The temperature evolution in the cavity should follow the bulk temperature (CAV), using the measured temperature by the plate thermocouples (PT), see Figure 6(c, d, e), assuming the heat transfer by convection and radiation inside the cavity. The density of the mesh used for thermal analysis in solids is

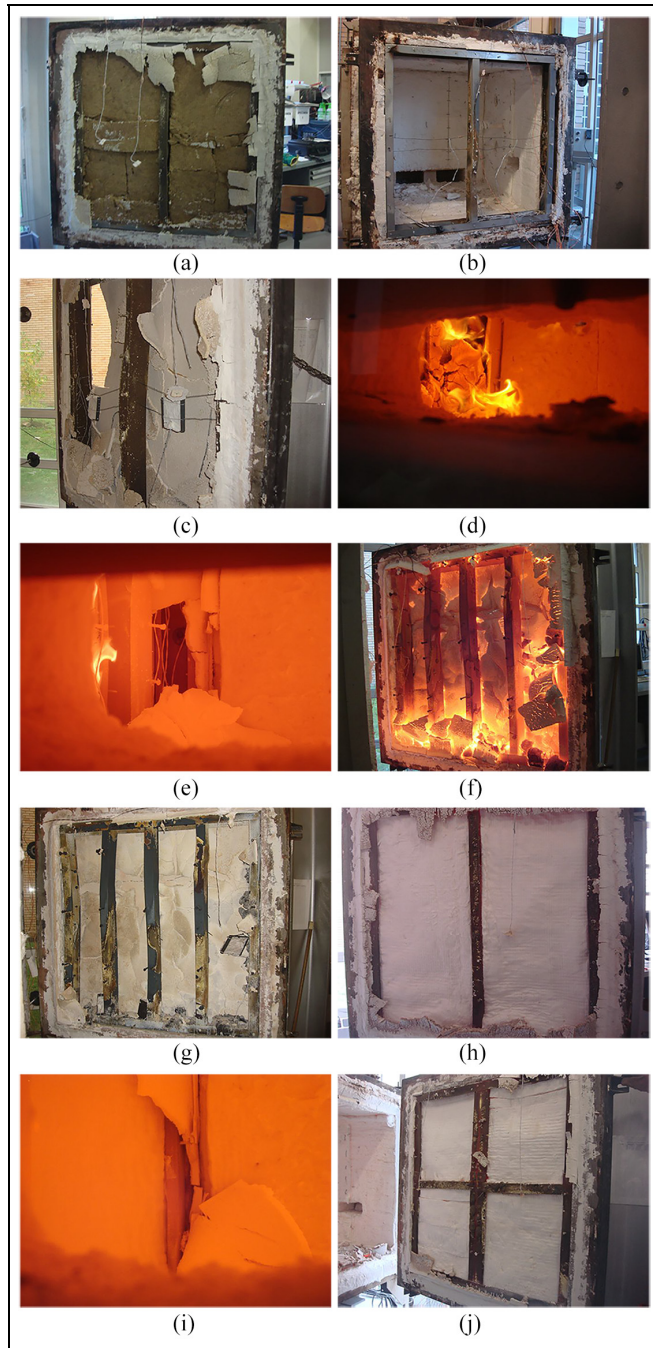


Figure 5. Wall specimens during and after being tested: (a, b) Specimen 10; (c) Specimen 11; (d) Specimen 12; (e) Specimen 13; (f, g) Specimen 14; (h) Specimen 15; (i, j) Specimen 16.

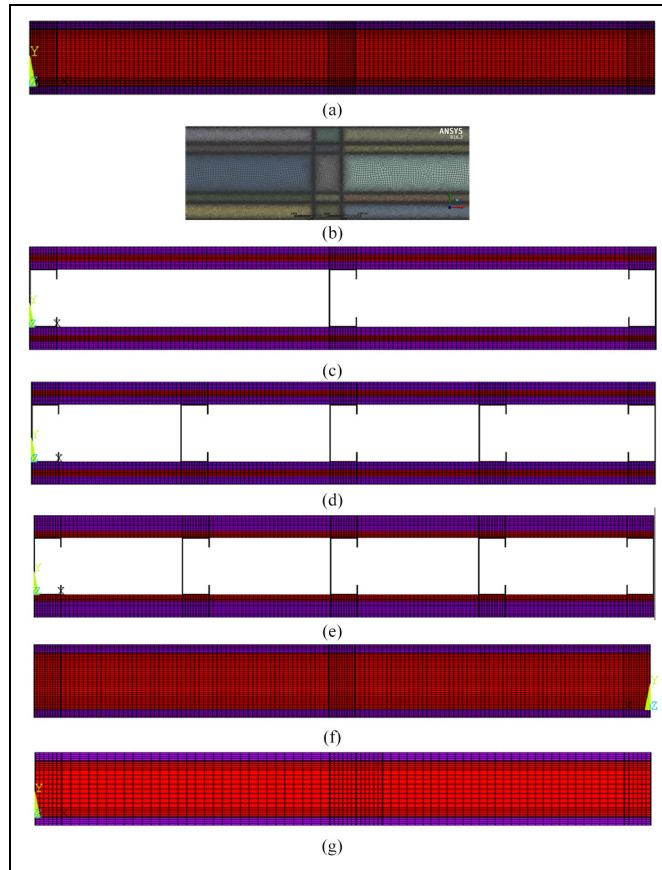


Figure 6. Finite elements and cells used for the simulations of the specimens: (a) Solution Method 2 for test Specimen 10, (b) Solution Method 1 for test Specimen 11, (c) Solution Method 3 for test Specimen 12, (d) Solution Method 3 for test Specimen 13, (e) Solution Method 3 for test Specimen 14, (f) Solution Method 2 for test Specimen 15 and (g) Solution Method 2 for test Specimen 16.

smaller in comparison with the cells used in FVM, nevertheless the thickness of the studs was divided into three finite elements as well. The mesh was defined based on a convergence test using calculation of the internal heat flow, with a minimum reference value of $1\text{E}-6$ and a tolerance value of 0.001.

One side of the wall was submitted to fire and the other side is assumed to remain in contact with room temperature. The boundary conditions are defined in accordance to EN 1991-1-2,²¹ assuming heat transfer by radiation (emissivity of fire $\varepsilon_f = 1$) and convection (convection coefficient $\alpha_c = 25 \text{ W/m}^2\text{K}$) in the exposed side and heat transfer by convection (convection coefficient $\alpha_c = 9 \text{ W/m}^2\text{K}$) in the unexposed side to include the radiation effect. The bulk temperature in the exposed side follows the standard ISO834.¹⁸ The room temperature of the unexposed side was considered equal to the initial temperature ($T_0 = 20^\circ\text{C}$), during all the simulation time.

For the tests with a composite panel (3 layer), Specimens 12, 13 and 14, the same boundary conditions were assumed, but an extra boundary condition was applied on empty cavity that follows the effect of the fire curve coming from the experimental results of each specimen (CAV) – H-FEM solution method. A convection inside the cavity was applied on all the lines that surrounds the cavity (convection coefficient $\alpha_c = 17.5 \text{ W/m}^2\text{K}$), and radiation on the same lines that surrounds the cavity (emissivity of fire $\varepsilon_f = 1$). This new convective coefficient should be considered as an average value for the entire simulation of the test. During the first part of the test, the integrity of the gypsum is maintained and a low value for the convective coefficient should be consider. After losing the integrity, the hot gases and flames are going to be inside the cavity region and the convective coefficient should increase (second part of the test). An average value for the convection coefficient, between 9 and 25 (natural and forced convection) is applied during all the tests. The value $17.5 \text{ W/m}^2 \text{ K}$ is a good approximation for this convective heat flow convection inside the cavity, during all the simulation process.

The thermal properties of all the materials were considered temperature dependent. Figure 7 depicts all the major properties that were used to solve the energy equation. The steel properties were retrieved from EN 1993-1-2¹⁹ and the gypsum properties were retrieved from the work developed by Mohamed Sultan.²² The thermal properties of the cork and OSB assumed the same type of temperature dependence in accordance to the reference material (softwood) in EN 1995-1-2,²³ but small modifications were applied to the properties of the cork (elimination of the specific heat peak value and adjustment of the conductivity and specific heat, based on the measured value at room temperature using the hot disc method).²⁴ The thermal properties for the Rockwool were obtained from Steinar Lundberg,²⁵ duly adapted to the corresponding material density 75 kg/m^3 . The emissivity of steel and cork was considered equal to 0.7,^{20,26} the emissivity of gypsum and OSB equal to 0.8.^{22,23} The thermal properties of the superwool Blanket plus, with 128 kg/m^3 , were obtained from Morgan Thermal Ceramics.^{27,28}

Numerical results

The temperature evolution is presented in Figure 8 for each simulation, collecting the average nodal temperatures in the same regions where the thermocouples were located. The difference between the hot flange (HF) temperature and the cold flange (CF) temperature is higher, for the Specimens 10, 15 and 16, due to the existence of insulation material in the cavity region. This fact is also verified in the numerical simulations because the perfect contact model between materials was assumed. This perfect contact is responsible for a heat flow decrease in the web of the steel, from the hot flange to the cold flange, during the heating process.

The insulation materials (rockwool and superwool) have higher thermal conductivity than the fluid (air) in the cavity (Specimen 11). This justifies the higher conduction resistance of the air in comparison to these materials. The heat flow by conduction is the only mean of heat transfer in the solid-filled cavity (Solution Method 2), while radiation and convection are also considered for the simulation of the fluid cavity (Solution Method 1) and empty cavity (Solution Method 3). The Specimens 12, 13 and 14 present similar trends due to the existence of similarity composite solution for the LSF wall (absence of insulation material in the cavity and the existence of a composite layer for the steel protection).

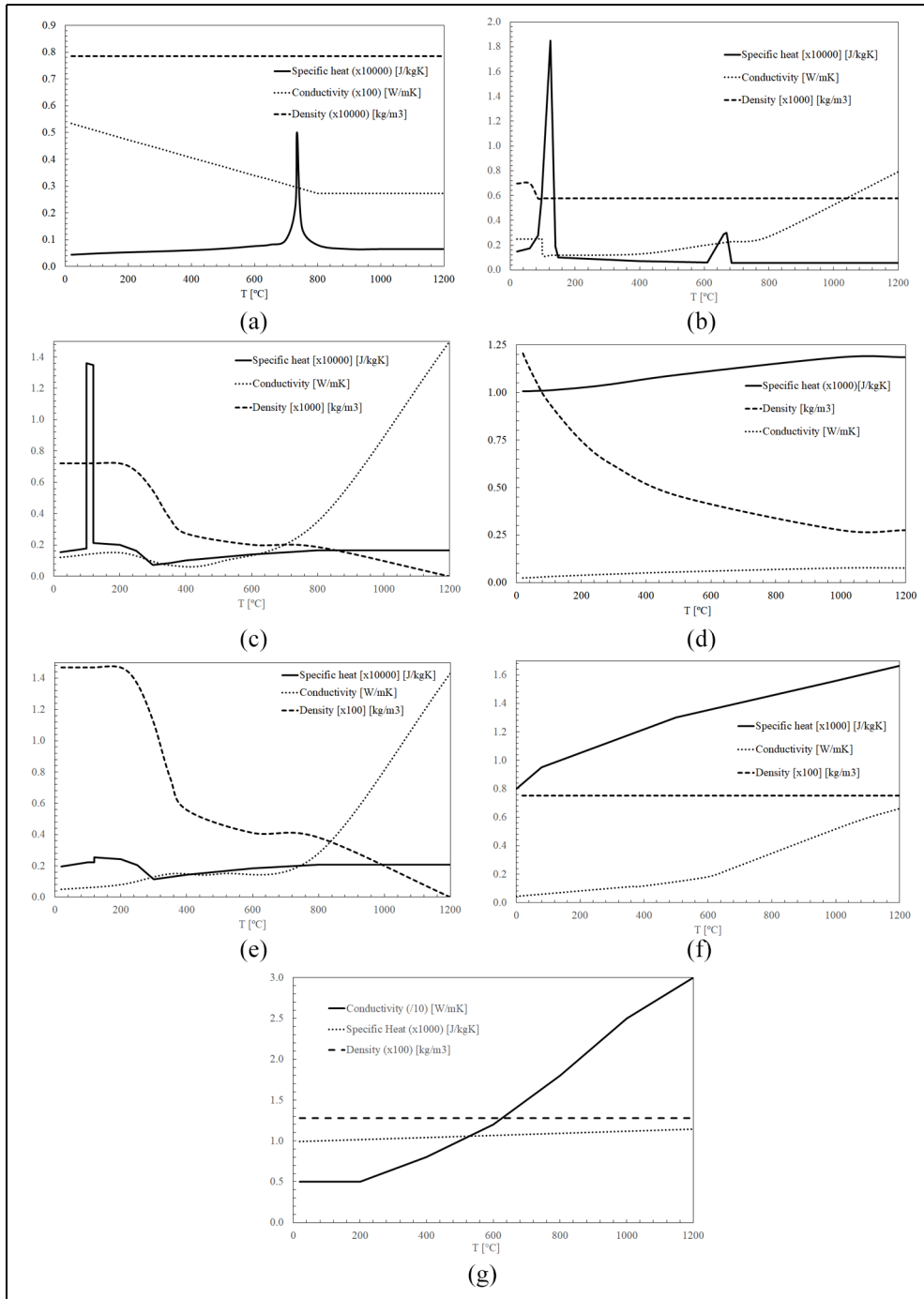


Figure 7. Thermal properties for all the materials involved in thermal simulation: (a) steel, (b) gypsum, (c) OSB, (d) air, (e) cork, (f) rockwool and (g) superwool.

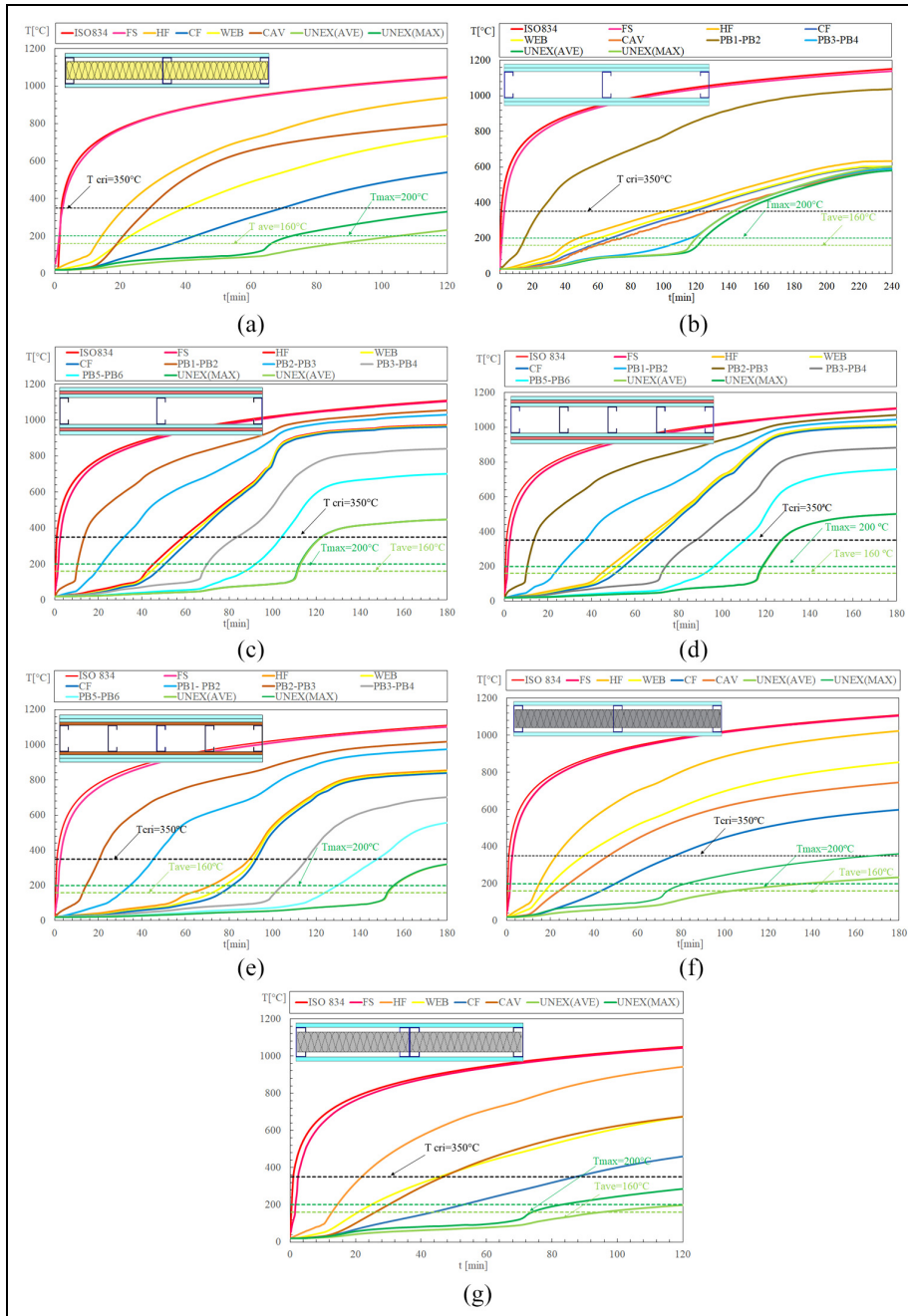


Figure 8. Time history for temperature during the simulation of all the tests: (a) results of simulation test Specimen 10 (Solution Method 2), (b) results of simulation test Specimen 11 (Solution Method 1), (c) results of simulation test Specimen 12 (Solution Method 3), (d) results of simulation test Specimen 13 (Solution Method 3), (e) results of simulation test Specimen 14 (Solution Method 3), (f) results of simulation test Specimen 15 (Solution Method 2) and (g) results of simulation test Specimen 16 (Solution Method 2).

Table 3. Comparison between numerical simulation and experimental results.

Specimen ID	DT _{max} Test (min)	DT _{max} Simulation (min)	Difference (%)	DT _{ave} Test (min)	DT _{ave} Simulation (min)	Difference (%)
10	79	72	8	95	86	10
11	114	121	7	115	122	8
12	112	112	0	113	112	0
13	122	118	3	127	117	7
14	145	151	4	146	153	4
15	95	83	12	115	105	8
16	86	83	3	100	95	5

The numerical results for the unexposed temperature were calculated with a significant number of nodal temperatures (minimum of 45 nodal temperatures). The main difference between the experimental results and the numerical results can be justified by the localised effect of a crack, opening or the ignition of the combustible material. The biggest temperature difference in the unexposed surface, between UNEX (AVE) and UNEX (MAX), is obtained for the models with insulation materials in the cavity region (simulation of Specimens 10, 15 and 16).

Comparison between the experimental and numerical results

The Table 3 shows the critical time obtained from experimental results and the critical time determined from numerical simulation. The differences are between 0% and 12%. The comparison was made following the temperature criteria used for rating the fire resistance by insulation, using the maximum temperature criterion (DT_{max}) or average temperature criterion (DT_{ave}) in the unexposed surface. The failure usually occurs in the back side of the studs and similar behaviour was detected during simulations. The results are presented in completed minutes in the Table 3.

The results agree well, not only for the critical time, but also when comparing the temperature history for the steel (HF, WEB, CF), for the exposed gypsum plate FS (exposed side), for the unexposed gypsum plate (UNEX), for the cavity (CAV), or for the interface between layers (PB_i–PB_j).

Figure 9 compares the temperature history from the unexposed side, using the maximum and average temperature. The specimens with higher differences are those using insulation materials (FEM). The model using H-FEM looks to be a good approximation for validation of the experimental results because it can reproduce, approximately, the main fire events during the test.

Conclusion

This work presented a summary of a detailed fire resistance analysis of seven LSF non-load-bearing walls, based on both experimental tests and numerical simulation. The LSF walls were tested in accordance with standards and the fire resistance was determined for the insulation criterion (I).

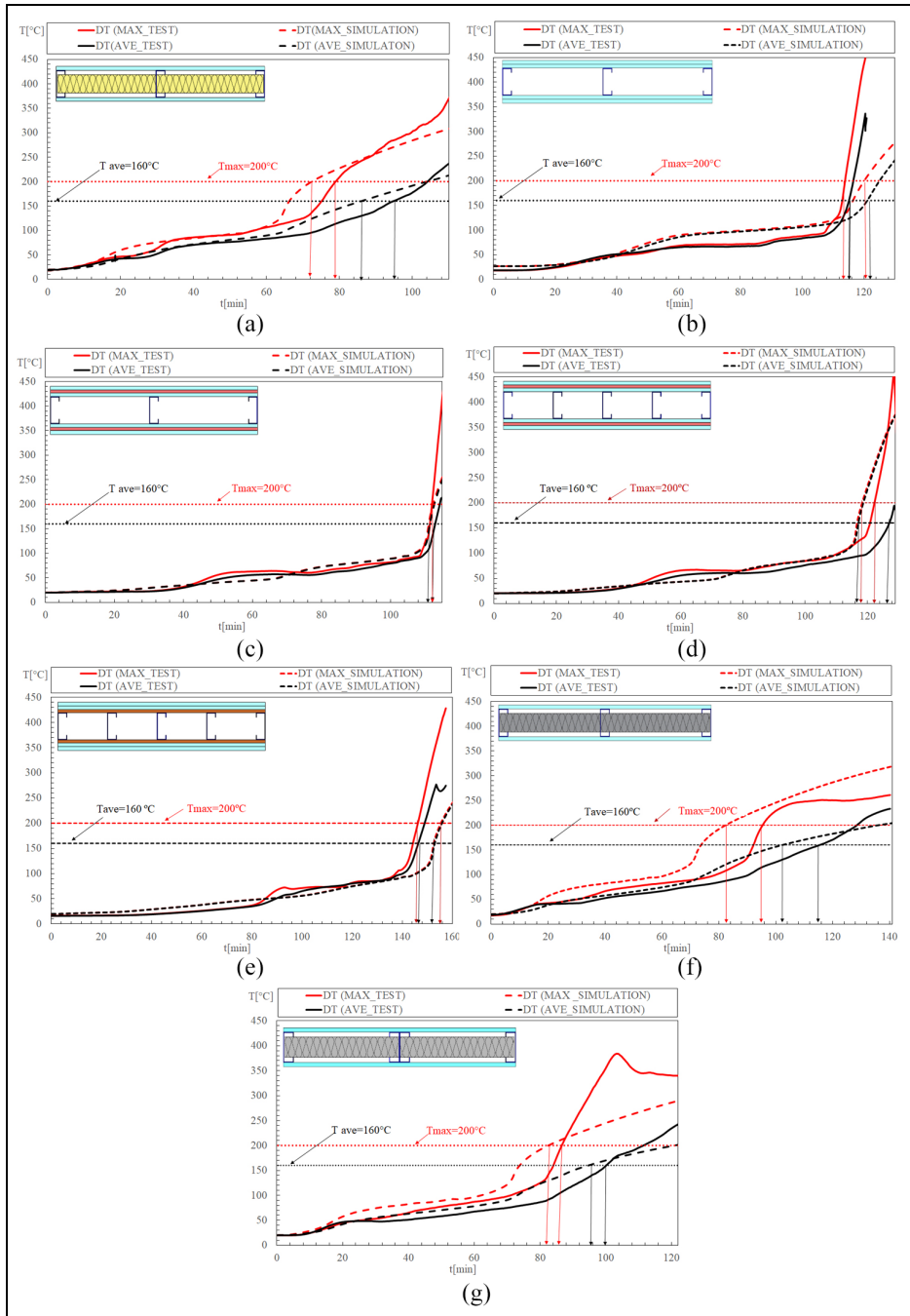


Figure 9. Temperature history comparison for the unexposed temperature (maximum and average): (a) time history comparison of Specimen 10, (b) time history comparison of Specimen 11, (c) time history comparison of Specimen 12, (d) time history comparison of Specimen 13, (e) time history comparison of Specimen 14, (f) time history comparison of Specimen 15 and (g) time history comparison of Specimen 16.

Different solution models were used to validate the experimental tests, using the FVM (Solution Method 1) and FEM (Solution Method 2). The hybrid solution method (H-FEM, Solution Method 3) can be used to predict the fire resistance of partition walls, taking into consideration the heat transfer by convection and radiation inside the cavity. This solution method requires an extra temperature measurement for the evolution of the bulk temperature in the cavity and the selection of the appropriate heat flow coefficients. This measurement is of extreme importance to account for all the major events that may occur during tests (cracks of materials, ignition and the heat release developed by combustible materials). The difference between the results, obtained for the fire resistance criteria (I), are between 0% and 12%, being the best approximation achieved with H-FEM. The H-FEM solution method requires previous experimental measurement for the calculation of the fire resistance of LSF walls. Different types of composite layer and single layer were tested to protect the LSF structure, enabling the calculation of the typical bulk temperature in the cavity. The bulk temperature evolution depends on the type of the LSF and on the number and type of the protection layers. This bulk temperature approximation can be used for the simulation of similar LSF walls with different geometric dimensions.

The fire resistance of the LSF walls increases with the number of studs and also with the thickness of the protection layers. It was clearly observed that the insulation of cavities brings relevant improvements to fire resistance, but doubling the number of gypsum plates looks to compete with the LSF wall with insulation material in the cavity. The fire performance of two gypsum layers LSF wall (Specimen 11) was better than using one single layer with cavity insulation material (Specimens 10, 15 and 16).

Specimen 14 presents the higher fire resistance (I), mainly due to the higher stiffness of the OSB. This higher stiffness is responsible to support any out-of-plane displacement of the gypsum boards, preventing the falling down of the plates (visual observation from experimental test), helping the gypsum boards to keep their thermal insulation effect for longer time. The superwool (higher density), seems to be the best insulation material to be applied in the cavity, in comparison with Rockwool (low density). This observation is supported by the fire resistance comparison of Specimens 10 and 15, when using the same LSF structure.

Acknowledgments

Special thanks are due to the companies: Amorim Composites, FALPER/Fibroplac, F. Pereira building Materials and Normago.


Declaration of conflicting interests

The author(s) declared no potential conflicts of interest with respect to the research, authorship and/or publication of this article.

Funding

The author(s) received no financial support for the research, authorship and/or publication of this article.

ORCID iD

Seddik M Khetata  <https://orcid.org/0000-0003-1524-5249>

References

- EN 1363-1:2012. Fire resistance tests part 1: general requirements.
- EN 1364-1:2015. Fire resistance tests for non-loadbearing elements. Part 1: walls.
- Chajes A, Britvec S and Winter G. Effects of cold-straining on structural sheet steels. *J Struct Div* 1963; 89(2): 1963.
- Son BC and Shoub H. *Fire endurance tests of double module walls of gypsum board and steel studs* (Report). Washington, DC: National Bureau of Standards, 1973.
- Schwartz KJ and Lie TT. Investigating the unexposed surface temperature criteria of standard ASTM E119. *Fire Technol* 1985; 21(3): 169–180.
- Alfawakhiri F and Sultan MA. Fire resistance of loadbearing LSF assemblies. In: *Proceedings of the 15th international specialty conference on cold-formed steel structures*. St. Louis, MO, 2000, pp. 545–561, <http://www.scopus.com/inward/record.url?eid=2-s2.0-3042660153&partnerID=40&md5=c0c10ef1d600f8e6810705e9bc895af7>
- Ghazi Wakili K and Hugi E. Four types of gypsum plaster boards and their thermophysical properties under fire condition. *J Fire Sci* 2009; 27(1): 27–43.
- Nassif AY, Yoshitake I and Allam A. Full-scale fire testing and numerical modelling of the transient thermo-mechanical behaviour of steel-stud gypsum board partition walls. *Construct Build Mater* 2014; 59: 51–61.
- Vallée J. *Reliability of fire barriers*. Lund: Faculty of Engineering Department, Lund University, 2016.
- Dias Y, Keerthan P and Mahendran M. Fire performance of steel and plasterboard sheathed non-load bearing LSF walls. *Fire Safe J* 2019; 103: 1–18.
- Piloto PAG, Khetata MS and Gavilán ABR. Fire performance of non-loadbearing light steel framing walls – numerical simulation. In: *Proceedings of the 7th international conference mechanics and materials in design*, Albufeira, 11–15 June 2017, pp. 1603–1610. Porto: INEGI/FEUP.
- Khetata M, Fernandes L, Marinho C, et al. Fire resistance of non-loadbearing light steel framing walls: numerical validation. In: *Proceedings of the XI Portuguese congress on steel and composite construction (CMM)*, Coimbra, 21–22 November 2017, pp. 853–62. Porto: Portuguese Association for Steel and Composite Construction.
- Piloto PAG, Khetata MS and Gavilán ABR. Fire performance of non-loadbearing light steel framing walls- numerical and simple calculation methods. *Int J Sci Technol* 2017; 3(3): 13–23.
- Piloto PAG. Fire resistance of cold-formed steel walls with composite panels: results from insulation rating (I) and loadbearing prediction rating (R). *Metálica Int* 2018(7): 12–17.
- Piloto PAG, Khetata MS and Gavilán ABR. Loadbearing capacity of LSF walls under fire exposure. *Int J Sci Technol* 2018; 4(3): 104–124.
- ANSYS®. Academic research mechanical (Release 18.2), <https://www.ansys.com/academic/terms-and-conditions>
- Piloto P, Khetata M and Gavilán A. Fire resistance tests of non-loadbearing LSF walls. In: *Proceedings of the 2nd conference on testing and experimentations in civil engineering (TEST&E)*, Porto, 19–21, February 2019, pp. 429–440. Porto: RELACRE – Associação de Laboratórios Acreditados de Portugal. ISBN 978-972-8574-49-9. DOI: 10.5281/zenodo.3355354.
- ISO 834-1:1999. Fire-resistance tests – elements of building construction – part 1: general requirements.
- Khetata SM, Piloto PAG and Gavilán ABR. Non-loadbearing light steel framing walls under fire. In: *Proceedings of the 5th Iberian-Latin-American congress on fire safety (CILASCI 5)*, ALBRASCI (Luso Brazilian Association for Fire Safety), eds. Porto, Portugal, 15–17 July 2019, pp. 169–185. ISBN: 978-989-97210-4-3.
- EN 1993-1-2:2005. Eurocode 3: design of steel structures – part 1-2: general rules – structural fire design.
- EN 1991-1-2:2002. Eurocode 1: actions on structures – part 1-2: general actions – actions on structures exposed to fire.
- Sultan MA. A model for predicting heat transfer through noninsulated unloaded steel-stud gypsum board wall assemblies exposed to fire. *Fire Technol* 1996; 32(3): 239–259.
- EN 1995-1-2:2004. Eurocode 5 – design of timber structures part 1-2: general – structural fire design.
- ISO 22007-2:2015. Plastics – determination of thermal conductivity and thermal diffusivity – part 2: transient plane heat source (hot disc) method.
- Lundberg S. Material aspects of fire design (TALAT Lectures 2502), 1994, <http://core.materials.ac.uk/search/detail.php?id=2178>
- Martinez I. *Thermo-optical properties*. Madrid: ETSIAE – Polytechnic University of Madrid, Spain, 2019.
- Data sheet superwool blanket. In: *Thermal ceramics*, 2016, pp. 1–3, http://www.morganthermalceramics.com/media/3993/cera_blankets-data-sheet-english.pdf
- Superwool plus insulating fibre. In: *Thermal ceramics* (section 1.6). Morgan Advanced Materials, 2016, pp. 29–34, http://www.morganthermalceramics.com/media/1503/14_third_party_testing_factsheet_sept_14-eng.pdf

Author biographies

Seddik M Khetata is a PhD student, enrolled in the PhD programme Applied Physics and Technology, from the University of Salamanca (USAL), Patio de Escuelas, 1, 37008, Salamanca, Spain.

Paulo AG Piloto is a coordinator professor at the Department of Applied Mechanics, Polytechnic Institute of Bragança (IPB), Portugal, having performed other professional activities in business and university environment and develops the research activity in the field of fire and structural engineering.

Ana BR Gavilán is a professor at the Mechanical Engineering Department, University of Salamanca (USAL), Spain, and develops the research activity in the field of fire and materials.